J Mater Sci (2008) 43:2895–2907
DOI 10.1007/s10853-007-1876-3

The nucleating effect of exfoliated graphite nanoplatelets and their influence on the crystal structure and electrical conductivity of polypropylene nanocomposites

Kyriaki Kalaitzidou · Hiroyuki Fukushima · Per Askeland · Lawrence T. Drzal

Received: 11 November 2006 / Accepted: 23 May 2007 / Published online: 25 October 2007

Abstract The focus of this research is to investigate how exfoliated graphite nanoplatelets, xGnP^{TM}, (graphene sheets ~10 nm thickness, ~1 μm diameter), a nanomaterial developed by the Drzal group, affects the crystallization of semicrystalline thermoplastics i.e., polypropylene (PP). In addition, this study explores how the presence of xGnP in combination with the processing conditions used to make the xGnP-PP nanocomposites alter the crystal structure and electrical conductivity of these systems. The nanocomposites are fabricated (i) by melt mixing followed by injection molding and (ii) by coating PP powder with xGnP with sonication in isopropyl alcohol followed by compression molding. PP was found to nucleate on the graphene surface of xGnP that is an effective nucleating agent for the β-form of PP crystals at low concentrations. The β-form of PP crystals has higher impact strength and toughness compared to the more common occurring α-form. It is found that the aspect ratio and concentration of xGnP combined with the crystallization conditions can be used to engineer the crystal structure such as the population and size distribution of PP spherulites and alter the electrical conductivity of xGnP-PP nanocomposites. The reason is that the presence of many small spherulites nucleated by the xGnP disrupts the percolated network formed by the conductive particles and thus increases the concentration required to reach conductivity and alters the conductivity value.

K. Kalaitzidou (✉)
Department of Polymer Science and Engineering,
University of Massachusetts, Amherst, MA 01003, USA
e-mail: kalaitzi@data.pse.umass.edu

H. Fukushima · P. Askeland · L. T. Drzal
Department of Chemical Engineering and Materials Science,
The Composite Materials and Structures Center, Michigan State
University, East Lansing, MI 48823, USA

Introduction

The crystallization behavior of a polymer, i.e., degree of crystallinity, crystallization temperature and rate, and size or type of crystallites formed is a combined result of the processing method/conditions and the presence of a second phase. Any change in the crystallization behavior of the polymer will be reflected in the mechanical and thermal properties of the composites as well as in the barrier properties since permeation rates through a polymer film strongly depend on its crystallinity [1, 2].

Typically, thermoplastic polymers crystallize into a specific crystal form. In the case of isotactic PP there are different packing geometries of the PP helices that lead to four well-known crystal structures: monoclinic (α), trigonal (β), triclinic (γ), and smectic (δ) depending on the melting history, crystallization temperature, pressure and cooling rate as well as presence of a foreign material [3, 4]. The most common is the α-form. However, it has been reported that the less common β-form has higher impact strength and toughness that are attributed to its peculiar lamellar morphology [5], the formation of an enlarged plastic zone [6] and the strain-induced β–α transition during mechanical deformation [7]. Based on TEM observations [8], the β crystals consist of thicker lamellae compared to those of α-form (20 nm for β-form versus 10 nm for the α-PP).

It is documented that nanoreinforcements can nucleate and promote the formation of less common crystal forms such as in the case of clay-Nylon 6 [9] and clay-PP [5–7] systems where the presence of clays favors the formation

of the less common γ-form and β-form crystals, respectively. Considering that in the case of PP the β-form has higher impact strength and toughness [5–7] it is concluded that clays enhance the mechanical properties of PP not only due to the reinforcing effect but also because they induce polymorphism (more than one crystal-form). Similar studies on the crystal polymorphism induced by clays in nylon-6-clay indicate that the addition of clay increases the crystallization rate, orients the crystallites and acts as a template for epitaxial crystallization to the γ-phase, instead of the normally dominate α-phase, to the point where crystallization is no longer spherulitic [10–12].

In addition to clays, carbon nanotubes, even at low concentrations, also act as nucleating agent for PP increasing the crystallization temperature and rate of the neat polymer and resulting in smaller crystallites with a narrower size distribution [13]. It has also been reported that addition of octadecylamine functionalized SWNTs in PP at a loading of 0.6 wt% promotes the growth of the β-crystal form at the expense of α-form, [14]. A saturation effect of the preferable β-crystal form nucleation at higher [>5 wt%] SWNT content [15] is attributed to the fact that there is not enough polymer to intercalate between the SWNTs, thus limiting dispersion and restricting the nanotube surface that is available for crystal nucleation.

Graphite, which can be an alternative to clays and carbon nanotubes since it combines the platelet structure and low price of clays and the superior thermal and electrical properties of carbon nanotubes, is also expected to alter the crystallization behavior of polymers. The only study reported on the nucleating effect of graphite indeed confirms that graphite promotes the nucleation of the less preferable β-form crystals in PP [16]. However, due to the presence of graphite oxide and maleated PP that were used as interface modifiers, the effect of graphite, which is among the most common nanoreinforcements used [17], on the crystallization of polymers and thus on other nanocomposite properties is not well established.

In case of electrically conductive nanoreinforcements, crystallization can (in addition to the mechanical and barrier properties) alter the electrical properties of nanocomposites such as electrical conductivity and percolation threshold, defined as the minimum volume content of the reinforcement above which the composite becomes electrically conductive. A low percolation threshold is desirable in order to achieve good processability, low cost and satisfactory mechanical performance.

The majority of the studies on electrically conductive composites focuses on how the electrical conductivity and percolation threshold are affected by various factors such as the volume fraction, distribution, size and shape [18–20], orientation and spacing of the filler particles within the polymer matrix [21, 22] as well as the fabrication method and conditions of the composites [18, 23–28]. In addition, the crystallinity of the matrix is also an important factor since in a highly crystalline matrix the formation of the continuous conductive path is easier compared to a less crystalline polymer where the higher amorphous portion may result in more homogeneous particle distribution [29] or encapsulation of the particles. However, the effect of other crystallization characteristics such as type of crystal forms, number and size distribution of spherulites on the electrical properties of polymer composites has never been investigated.

The focus of this research is to determine how xGnP affects the crystallinity of polypropylene and understand how the crystallinity relates to the electrical properties of xGnP-PP composites. The goal is to combine the obtained knowledge in order to be able to engineer the crystal structure and lead to composites with desired properties. This is accomplished by altering the processing conditions (and thus the crystallization behavior of the matrix) and determining the electrical properties of the xGnP-PP nanocomposites. The objectives are:

- Determine the effect of xGnP on the crystallite size, crystallization temperature and rate and crystal polymorphism of neat PP as a function of the xGnP aspect ratio and concentration by means of DSC, optical microscopy and XRD.
- Determine the relationship between the crystallization behavior of PP in the presence of xGnP and mechanical properties of xGnP-PP composites i.e., impact strength.
- Investigate how compounding (melt-mixing versus coating PP powder with xGnP) affects the crystallinity of the nanocomposites.
- Study the effect of PP crystallization on the electrical conductivity and percolation threshold of xGnP-PP nanocomposites as a function of xGnP's aspect ratio and concentration.

Experimental

Materials

Powdered polypropylene (Basell, Pro-fax 6301: melt flow index 12 g/10 min, ASTM D1238) was used as the matrix for all composite specimens prepared in this work. This material was chosen as a representative of polyolefins, which are the most widely used thermoplastics due to their well-balanced physical and mechanical properties, easy processing and recycle characteristics which combined with their low cost makes them a versatile material [30, 31]. In addition, PP has a lower density, in comparison to other engineering thermoplastics, allowing for potential

weight reductions along with excellent moisture barrier properties and good optical properties due to its higher crystallinity [30]. Finally, PP due to its non-polar nature can be used as a model to provide insight into the interaction between xGnP and other semi-crystalline polymers.

The exfoliated graphite nanoplatelets are developed in the Drzal group. The starting material for xGnP is a sulfuric acid-based intercalated graphite [32], which is exfoliated according to a proprietary process using a microwave oven, a cost and time effective exfoliation process initially proposed by Fukushima [33]. The microwave radiation couples to the conductive graphite and rapidly raises its temperature, the entrapped intercalants vaporize causing the graphite flake particles to undergo significant expansion ($\sim$500 times). The result of this exfoliation process is the formation of a worm- or accordion-like expanded structure that is broken down to individual graphite nanoplatelets using an ultrasonic processor. The diameter of xGnP depends on the time of pulverization and can be as small as 15 microns, a product called xGnP-15. The diameter can be further reduced using a vibratory mill, resulting in nanoplatelets with the same thickness but with diameter less than 1 μm (xGnP-1) as shown in Fig. 1a. The thickness of xGnP was studied by TEM. A representative image is presented in Fig. 1b, which shows two adjacent nanoplatelets, each consists of more than 10 graphene sheets. Taking into account that the basal plane distance of graphite is 0.335 nm [34] it is estimated that the average thickness of the graphite nanoflakes is $\sim$5 nm with a distribution of platelets having thicknesses expected in the nanometer range.

Processing

The basic fabrication method used in this project is melt-mixing due to its simplicity and compatibility with existing polymer processing techniques such as extrusion, injection molding and compression molding. The nanocomposites were fabricated in a DSM Micro 15 cc Compounder, (vertical, co-rotating twin-screw microextruder), at 180 °C for 3 min at a screw speed of 200 rpm. The injection-molded samples were made using a Daca Micro Injector. The cylinder temperature was 180 °C and the mold temperature used was 80 °C. An injection pressure of 160 psi was used. The operating conditions used in both the extruder and the injector were optimized using 2^3 factorial experimental design with respect to the flex strength and modulus of 3 vol% xGnP-1/PP nanocomposites [35].

A second compounding method used is coating the PP powder with xGnP followed by compression molding. This method, as developed in the Drzal group, results in better dispersion of xGnP within the PP matrix and also in composites with lower percolation threshold [35]. The xGnP is dispersed in isopropyl alcohol (IPA) by sonication for 1 h at room temperature. The PP powder is added to the solution and sonication is continued for 0.5 h. Finally, the solvent is evaporated at 80 °C resulting in complete coverage of the powder particles with the xGnP. The main advantage of this method is that sonication breaks down the xGnP agglomerates and the thick xGnP-IPA solution covers the PP particles very efficiently resulting in a homogeneous xGnP coated PP powder that is used for compression molding.

The compression-molded samples were made using the xGnP-coated PP powder. The conditions used are 200 °C for 20 min with no pressure applied followed by 200 °C for 20 min under $\sim$137 MPa psi. During the compression molding vacuum was applied to remove any trapped air.

Characterization techniques

The degree of crystallinity, crystallization enthalpy (ΔH_c), crystallization temperature (T_c), melting enthalpy (ΔH_m) and melting temperature (T_m), were determined by DSC. The samples used were 5–10 mg and isothermal crystallization was studied using the following experimental conditions.

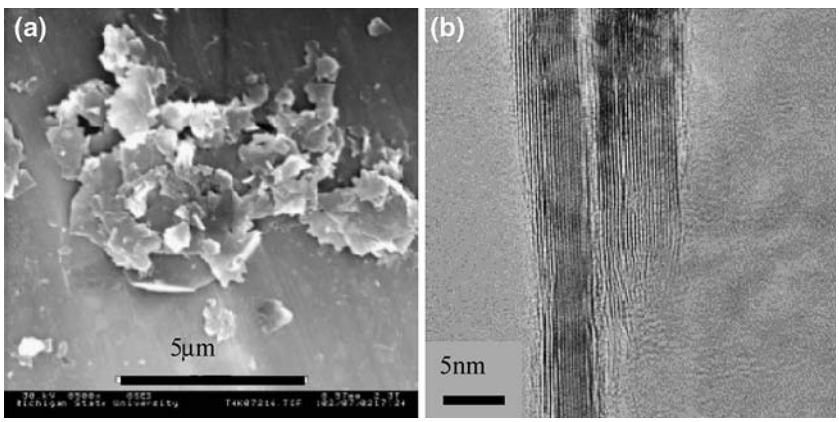

Fig. 1 (**a**) ESEM micrographs of exfoliated graphite nanoflakes xGnP-1 (*top view*, scale bar 5 μm) and (**b**) TEM images of xGnP-1, (*side view*, scale bar 5 nm)

The sample was heated to 220 °C at a rate of 30 °C/min. The thermal history of the sample due to prior processing was erased by maintaining isothermal condition for 10 min. Finally, the sample was cooled at 5 °C/min to –40 °C, held isothermally for 5 min and reheated at 5 °C/min to 220 °C. The data on the melting behavior was collected along this second heat cycle whereas the crystallization data was collected during subsequent cooling the sample to room temperature at 5 °C/min.

The degree of crystallinity was calculated using the following equation

$$\chi\% = \frac{1}{1 - \mathrm{wt}\%} \frac{\Delta H_C}{\Delta H_f^o} \quad (1)$$

where $\chi\%$ is the percent crystallinity of the matrix, wt% is the content of xGnP, and ΔH_f^o is the theoretical crystallization enthalpy of the matrix if it was 100% crystalline.

Non-isothermal and isothermal crystallization of xGnP-PP nanocomposites were studied using an optical microscope. A hot stage was used to initially heat the sample above the melting point in order to erase the thermal history. The sample was heated up to 220 °C at a rate of 20 °C/min, held isothermally at 220 °C for 10 min and then cooled to room temperature (for non-isothermal crystallization) or to the desired crystallization temperature (for isothermal).

The X-ray diffraction patterns of the nanocomposites were obtained using a Rigaku Rotaflex 200 B diffractometer employing Cu-Kα radiation (λ = 1.54056 Å) with a curved graphite monochromator. The operating setting of the X-ray was 45 kV and 100 mA. The diffraction patterns were collected from 10° to 50° (2θ) at a scanning rate of 1°/min with divergence and scatter slit of 1/2°. Information obtained by the XRD pattern includes the types of crystals that are present and the crystal size (thickness of the crystallite along the direction perpendicular to the reflecting plane), which can be estimated using the Scherrer formula [36] described in Eq. 2:

$$\text{Crystallite size} = K \times \lambda / \text{ FWHM} \times \cos\theta \quad (2)$$

where K is the crystal shape factor taken as 0.9, λ is the wavelength, and θ is the peak position.

The effect of processing conditions on crystallinity of xGnP-PP nanocomposites and consequently the electrical conductivity and percolation threshold was investigated by altering the cooling conditions during the compression molding of the samples. The samples were made by coating and compression molding. Two extreme cases were used during cooling, fast cooling at a rate of ~20 °C/min which was achieved by immersing the mold in dry ice and slow cooling at a rate of ~0.3 °C/min which was carried out by leaving the mold in the hot press, turning off the heat and letting the samples slowly cool down to room temperature overnight.

The resistivity of xGnP-PP was measured, as a function of cooling rate, xGnP concentration and aspect ratio, using impedance spectroscopy (Gamry, FAS2Ô Femtostat plug system and potentiostatic mode) by applying a two-probe method at room temperature. Samples with dimensions of $5 \times 3 \times 12$ mm^3 were cut from the middle portion of flexural bars, and the resistivity was measured along the thickness direction (5 mm). The two surfaces that were connected to the electrodes were first treated with O_2 plasma (10 min, 550 W) in order to remove the top surface layers which are polymer rich and then gold coated to a thickness of 1–2 nm to ensure good contact of the sample surface with the electrodes. It is expected that the contact resistance is similar throughout all the samples tested and although the accuracy may be off, the overall trends are still valid. In addition, the variation in contact resistance is taken into account in the standard deviation of the experimental data. The electrochemical impedance spectrum over a range of frequencies from 0.1 to 100,000 Hz of xGnP reinforced composites has been measured and the impedance value at 1 Hz is converted to conductivity by taking into account the sample dimensions. It is noted that in case of conductive materials the conductivity is invariable with frequency whereas the conductivity of insulators decreases with decreasing frequency.

Results and discussion

Effect of xGnP-1 and crystallization conditions on nucleation of PP

The crystallization of neat PP was monitored by optical microscopy and the results are shown in Fig. 2a–c. The time intervals (t = 0, 1 and 2 min) indicate how long the specimen was held at 130 °C. At t = 0 there are preexisting nuclei due to infusible heterogeneous particles (e.g., impurities or catalyst residues). As time proceeds spherulites form around these nucleating sites and keep growing. No secondary nucleation is observed. Figure 2d–f track the crystallization of 0.01 vol% xGnP-1/PP at 130 °C. The spherulites form and grow around the xGnP-1 particles, which is the first indication of the ability of xGnP to act as a nucleating agent.

When comparing the neat PP crystallization to the filled system, several striking differences are observed. First the rate of crystallization, the length of time it takes for the spherulites to cover the micrograph area, is much faster for the xGnP-1/PP (completion in less than 3 min) than the neat PP (completion in 20 min) as observed in Fig. 3. A more quantitative description of the crystallization rate is provided in Table 1. Figure 3 also reveals that the spherulites formed in the xGnP-1/PP system are almost 10 times smaller than those formed in neat PP and have a more irregular shape.

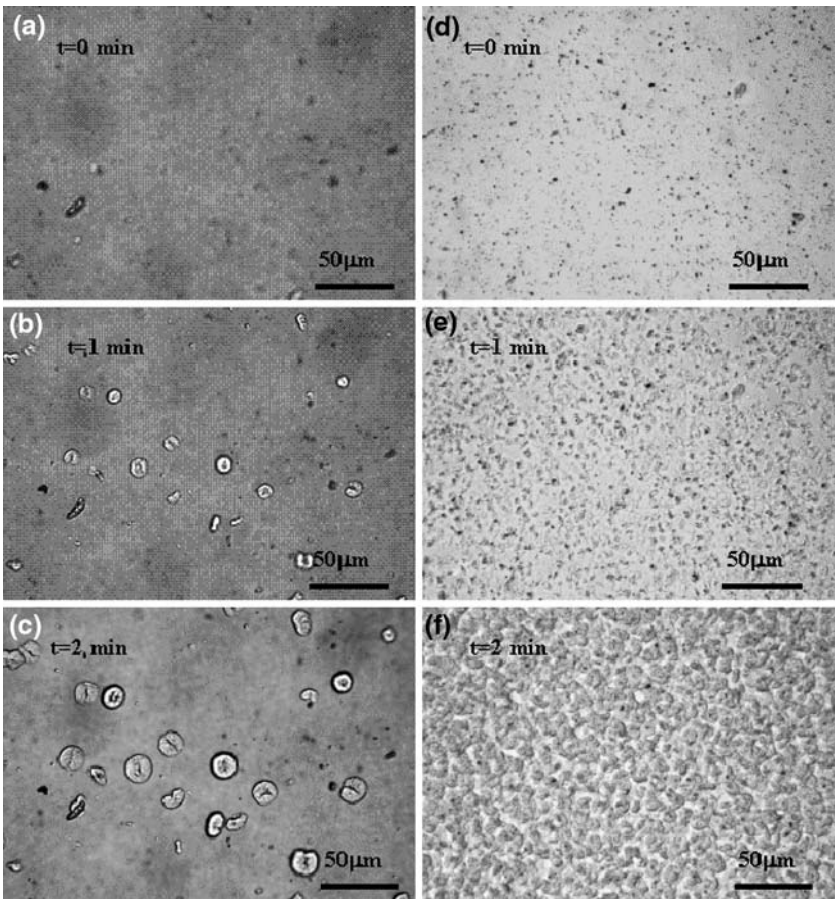

Fig. 2 Isothermal crystallization at T = 130 °C of neat polypropylene (PP), images (**a**) through (**c**), and of 0.01 vol% xGnP-1/PP, images (**d**) through (**f**). Viewing the images from left to right shows the difference in crystallization between PP and xGnP/PP at a given time whereas viewing them from top to bottom shows how crystallization evolves with time for PP (*left*) and xGnP-1/PP (*right*)

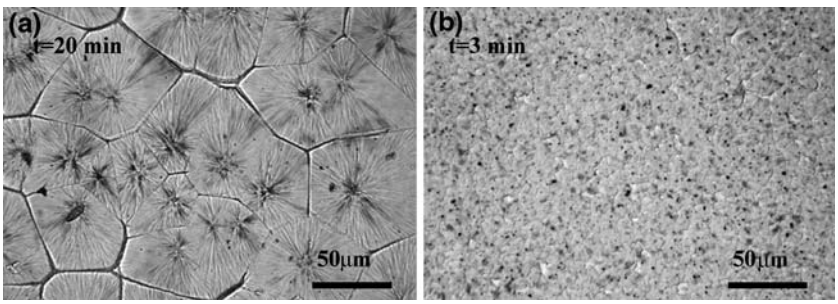

Fig. 3 Isothermal crystallization at 130 °C of (**a**) neat polypropylene (PP) at t = 20 min and (**b**) 0.01 vol% xGnP-1/PP at t = 3 min

Table 1 Crystallization rate of xGnP/PP for isothermal crystallization at T_c = 130 °C

Vol%	xGnP-15 (1/min)	XGnP-1 (1/min)
0	0.060 ± 0.004	0.060 ± 0.004
0.01	0.164 ± 0.008	0.193 ± 0.014
0.1	0.226 ± 0.011	0.299 ± 0.010
1	0.535 ± 0.027	0.381 ± 0.032

The crystallization rate (1/min), an average of three samples, calculated as the inverse of the time interval required for the completion of the crystallization during isothermal crystallization of xGnP/PP at T_c = 130 °C in DSC is presented in Table 1. Even at the low xGnP content of 0.01 vol% the crystallization rate of neat PP increases by a factor of ~3.

The crystallization of PP is also affected by the processing conditions. Increasing the temperature at which crystallization occurs results in fewer but larger and more spherical spherulites and lower crystallization rates. The condition under which the crystallization occurs, for example isothermally or nonisothermally, is equally important. In the case of isothermal crystallization, after the spherulites nucleate and grow at constant temperature they shrink during cooling to room temperature as a result of the thermal and residual stresses that were accumulated during the crystallization process. Fracture between

adjacent spherulites takes place as indicated by the black lines formed along the boundaries as shown in Fig. 4a. However, in the case of non-isothermal crystallization as shown in Fig. 4b, the spherulites nucleate and grow as the temperature decreases without fracture since the spherulites adjust their size/boundaries gradually during cooling. The non-isothermal crystallization of 0.01 vol% xGnP-1/PP starts at $\sim T_c = 120$ °C and is completed within few minutes at $T_c = 114$ °C.

A study on clay reinforced polyolefins [2] reports that nanoclays reduce the crystal shrinkage, indicating that nanoreinforcements can enhance the composite's mechanical properties through an additional mechanism of reducing the residual stress from shrinkage in addition to the reinforcing and the nucleating effect. In the case of neat polymer the shrinkage appears during recrystallization due to a high degree of crystallinity and the large density difference between the amorphous melt and the crystal phase [2]. The nanoreinforcements have a much lower coefficient of thermal expansion compared to the polymer and based on the observation that spherulites grow around/on the nanoplatelets it is concluded that the reduction of crystal shrinkage upon addition of nanoreinforcements is due to the constraint they impose on the polymer spherulites.

Effect of xGnP concentration and aspect ratio on nucleation of PP

In order to study the effect of xGnP concentration on the crystallization of PP, xGnP-15/PP samples at two different xGnP loadings of 0.01 and 0.1 vol% were crystallized isothermally at $T_c = 120$ °C in the hot stage under the optical microscope. The micrographs are shown in Fig. 5. The crystallization rate as well as the number of nucleation sites and consequently the number of spherulites increases with the xGnP-15 concentration while their size is reduced and their shape becomes irregular. The nucleation starts around the graphite nanoplatelets as indicated in Fig. 5a, d by the "bright" rings formed along the periphery of the xGnP-15. It is expected that this transcrystalline zone should also form in the case of xGnP-1. However this is difficult to document optically. Composites with larger graphite platelets, xGnP-100 at a loading of 0.3 vol%, were manufactured to verify the existence of the transcrystalline region. The sample was

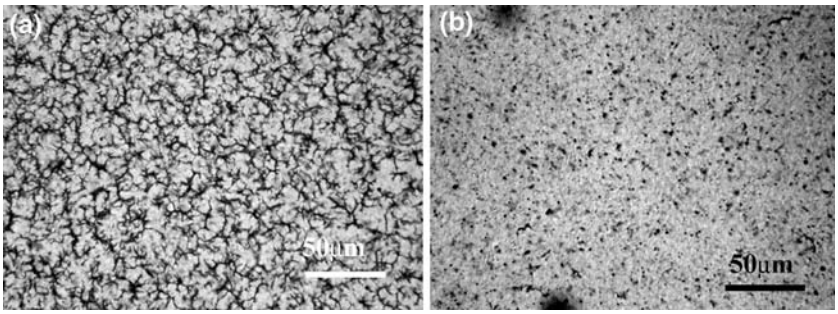

Fig. 4 Optical micrograph of 0.01 vol% xGnP-1/PP at $T = 28$ °C after (**a**) isothermal crystallization at $T_c = 130$ °C for $t = 20$ min and (**b**) non-isothermal crystallization

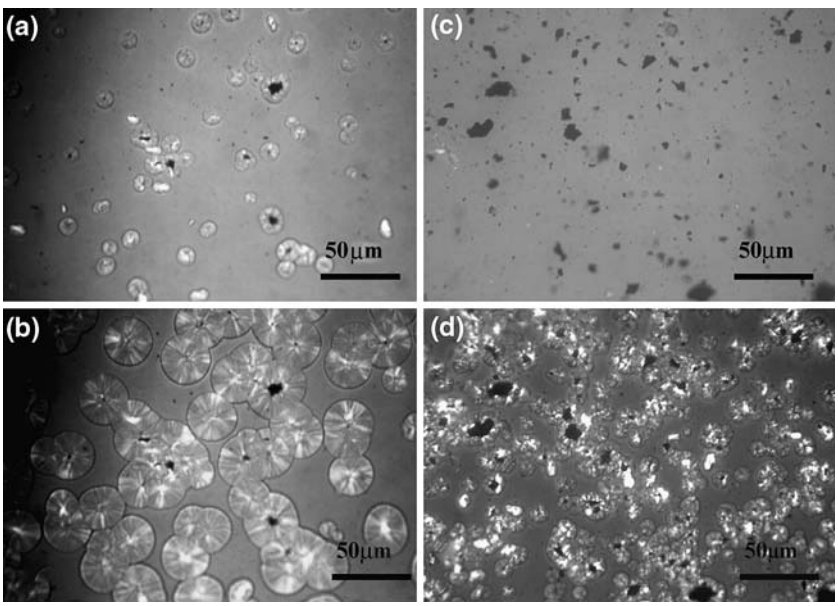

Fig. 5 Isothermal crystallization at $T = 120$ °C of 0.01 vol% xGnP-15/PP at (**a**) $t = 20$ s and (**b**) $t = 1$ min and of 0.1 vol% xGnP-15/PP at (**c**) $t = 0$ s and (**d**) $t = 20$ s

crystallized isothermally at T_c = 130 °C. Results are shown in Fig. 6. As the aspect ratio of xGnP increases the number of particles contained at a given xGnP volume decreases which means fewer nucleation sites and thus fewer but larger spherulites. Increasing the xGnP concentration has a similar effect as shown in Fig. 5.

In addition, the xGnP concentration and aspect ratio effect on the crystallization of PP was studied by DSC and XRD. As the xGnP content increases the crystallization initiates at higher temperatures (Fig. 7), which also confirms that xGnP acts as nucleating agent. Figure 7 also shows that the presence of xGnP does not have any significant effect on the total percent of crystallinity. The melting temperature, calculated as the minimum temperature of the exotherm melting peak provided by DSC, does not change. However, addition of xGnP alters the melting behavior evidenced by the melting peak becoming narrower and taller compared to the melting peak of neat polypropylene. This indicates that the crystals are becoming thinner and more homogeneous.

XRD was used to investigate the change in the crystal form of polypropylene due to addition of xGnP. The literature values for the characteristic XRD (Cu $K\alpha_{1,2}$) pattern of isotactic polypropylene and the corresponding crystallographic planes are summarized in Table 2. The crystalline forms of isotactic PP are α-monoclinic which is the most common, β-hexagonal (occurring under specific conditions such as temperature gradients, presence of shearing forces or β-nucleating agents), and γ-triclinic, which is the least commonly observed in low molecular weight PP [37].

The XRD patterns of melt mixed and injection molded xGnP-1/PP and xGnP-15/PP nanocomposites at various graphite loadings are shown in Figs. 8 and 9, respectively. Four peaks are present in the XRD pattern of neat PP (0 vol%) that correspond to the α-form crystals. The addition of only 0.01 vol% of xGnP-1 induces the formation of β-form crystals (at 2θ = 16° and 2θ = 21° shown by the arrows in Fig. 8), which disappear at higher xGnP loadings (1 vol%). It is also observed that the second PP peak at 2θ = 16.95° that corresponds to the $\alpha\langle 040\rangle$ plane dominates whereas in the case of neat PP all four peaks had similar height. Finally the addition of xGnP gives rise to a fifth PP peak at 2θ = 25° corresponding to the $\alpha\langle 060\rangle$ plane which is absent from the neat PP pattern.

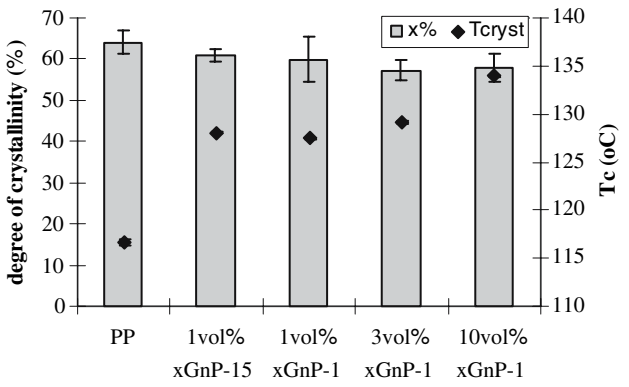

Fig. 7 Crystallization temperature and degree of crystallinity of xGnP-PP nanocomposites

Table 2 Characteristic XRD peaks and corresponding crystallographic planes of polypropylene (PP)

2θ	α-Form [37–39]	β-Form [39]	γ-Form [37]
13.84			(111)
14.08	(110)		
15.05			(113)
16		(300)	
16.95	(040)		
18.5	(130)		
20.07			(117)
21		(301)	
21.2	(111)		(202)
21.85	(041)		
21.88			(026)
25	(060)		
28	(220)		

Similar features are observed in the XRD pattern of xGnP-15/PP nanocomposites as shown in Fig. 9. Again, the second PP peak at 2θ = 16.95°, ($\alpha\langle 040\rangle$ plane) becomes stronger and the PP peak at 2θ = 25° corresponding to the $\alpha\langle 060\rangle$ plane, appears due to addition of xGnP-15. The presence of xGnP-15 also promotes the formation of

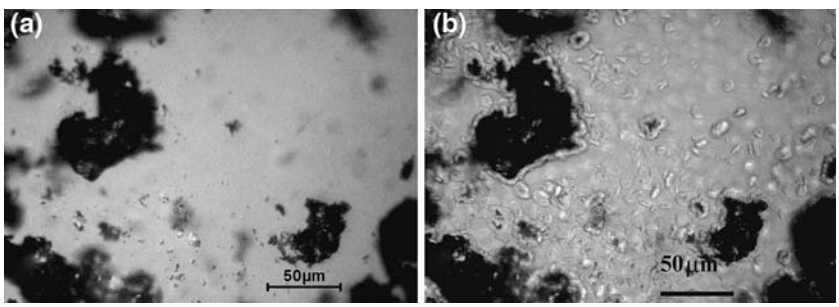

Fig. 6 Isothermal crystallization of 0.3 vol% xGnP-100/PP at T = 130 °C after (**a**) t = 0 min and (**b**) t = 1 min

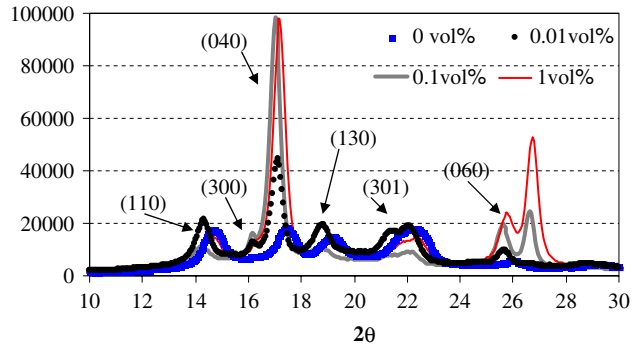

Fig. 8 XRD of xGnP-1/PP made by melt mixing and injection molding

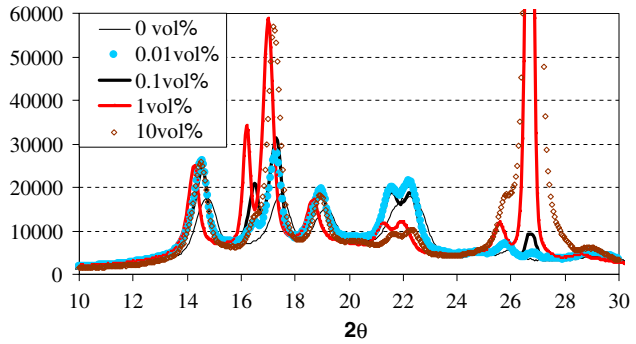

Fig. 9 XRD of xGnP-15/PP made by melt mixing and injection molding

β-form crystals with the β-form peak at $2\theta = 16°$ that corresponds to the $\langle 300 \rangle$ plane, dominating over the second β-form peak. It is noted that the three peaks that are strongly affected by xGnP correspond to the crystallographic planes of the general (00x) type, which also match crystallographically with the graphite $\langle 002 \rangle$ plane.

Similar findings are reported in a study [40] about the nucleation effect of talc on the crystallization of PP. It was observed that there is oriented crystallization of PP in the presence of talc as the mineral *c*-axis is merged with the PP *b*-axis (matching $\langle 001 \rangle$ plane of talc with the $\langle 010 \rangle$ plane of PP).

The above findings indicate that the xGnP nucleating efficiency in PP can be expressed as the change in the intensity ratio between the $\alpha\langle 040 \rangle$ and $\alpha\langle 110 \rangle$ reflections and that the onset of crystallization, which can be attributed to the alignment of few PP chains before the epitaxial growth, depends on the crystallographic nature of the substrate.

The differences between the XRD patterns of xGnP-1/PP and xGnP-15/PP are that in the case of xGnP-15 the β-form peaks are present even at higher xGnP-15 loadings and that the xGnP peak at $2\theta = 26.45°$ corresponding to the graphite's $\langle 002 \rangle$ plane [41], is more intense (with respect to the PP peaks) in composites containing xGnP-15. However, similar loadings of xGnP-1 generate a smaller peak as shown in Fig. 8. For example the β-peaks are not present above 1 vol% of xGnP-1 but they can still be detected in PP reinforced with up to 10 vol% of xGnP-15. This probably reflects the difference in size between the xGnP-1 and xGnP-15 and consequently, the number of graphite platelets that are present in each case for a given xGnP volume. It indicates saturation of the nucleating action at higher xGnP-1 content since there are not enough polymer chains to orient and align along all the graphite platelets that are present. Similar results of saturated nucleating effect were also reported for a SWCNT-PP system [15]. The stronger graphite peak in case of xGnP-15 is attributed to the presence of large oriented agglomerates due to poor dispersion and higher degree of alignment of xGnP-15 compared to xGnP-1 [35].

It has been reported that the β-form of PP has higher impact strength and toughness [3]. xGnP up to a loading of $\sim$1 vol% promotes the formation of β-crystals. It is expected that the impact strength of PP will increase upon addition of xGnP and that it will reach a maximum at the xGnP loading that corresponds to the saturation of the nucleating effect, which varies with the two types of xGnP used. Such a trend was observed for the impact strength data for xGnP-1/PP and xGnP-15/PP nanocomposites [35].

Effect of compounding on the crystallization of PP

The effect of the xGnP dispersion on the crystallization of PP was investigated by studying the XRD patterns of xGnP-PP nanocomposites made by (i) melt mixing and injection molding and (ii) coating the PP powder with xGnP, followed by melt mixing and injection molding. It is unavoidable to skip the melt mixing step since in order to do injection molding the premixed xGnP-PP powder has to be extruded. Both sizes of xGnP were used.

The XRD of the neat PP, the xGnP-1/PP and xGnP-15/PP made by the two compounding methods are shown in Fig. 10. The strong nucleating effect of the xGnP-1 can be seen by the increase of the three peaks that correspond to planes that match the crystallographic plane of graphite. These peaks are $\beta\langle 300 \rangle$ at $2\theta = 16°$, $\alpha\langle 040 \rangle$ at $2\theta = 16.95°$, and $\alpha\langle 060 \rangle$ at $2\theta = 25°$. These three peaks are stronger for the premixing and coating case compared to the melt mixing case for xGnP-1 as shown in Fig. 10. This is probably due to a more homogeneous distribution of xGnP-1. The trend is similar in case of xGnP-15.

Effect of matrix crystallization behavior on percolation threshold

In an effort to understand how the crystallization of PP affects the electrical conductivity and percolation threshold

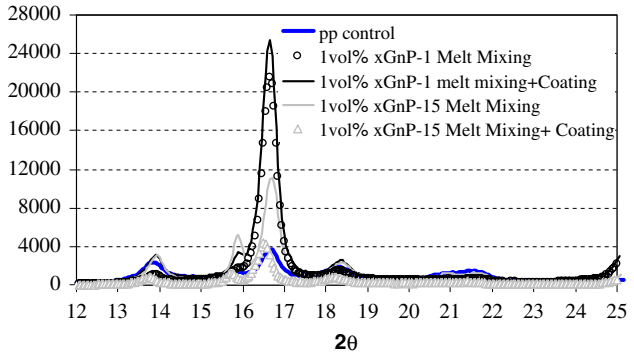

Fig. 10 XRD Pattern of xGnP/PP: effect of compounding

of xGnP/PP composites, samples were made by coating the PP powder with xGnP and compression molding. The crystallization of the matrix was altered by using different cooling rates after the molding was completed. Two extreme cases were used (i) fast cooling (fc) at a rate of ~20 °C/min and (ii) slow cooling (sc) at a rate of ~0.3 °C/min. Both xGnP-1 and xGnP-15 were used as reinforcements. The electrical conductivity of the nanocomposites was determined using the two-probe method described previously. The effect of cooling rate on the crystallinity was investigated by DSC and XRD.

The electrical conductivity of xGnP-1/PP and xGnP-15/PP as a function of xGnP concentration and the cooling rate is shown in Fig. 11. In both cases the slowly cooled composites have a lower percolation threshold (~0.1 vol% for xGnP-1 and between 0.3 and 0.5 vol% for xGnP-15). It is also observed that in case of xGnP-1 the effect of cooling rate becomes smaller as the xGnP concentration increases.

It is known that increasing the conductive filler's aspect ratio lowers the percolation threshold [42]. However, this is not observed with xGnP. In the coating method used for compounding, which results in PP powder coated by graphite platelets, the concentration (in terms of number of platelets in a given volume of xGnP) is more important than their size. For example, assume that both xGnP-1 and xGnP-15 agglomerate, as it is difficult to achieve

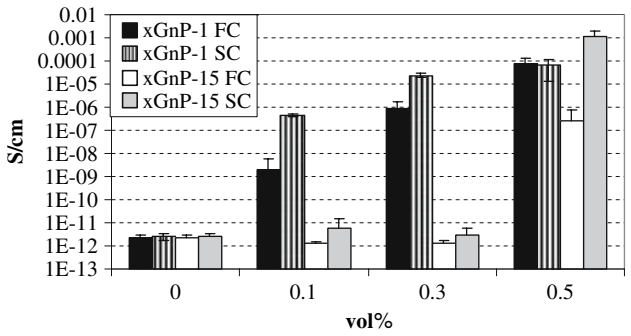

Fig. 11 Effect of cooling rate on the electrical conductivity of xGnP/PP

monolayer xGnP coverage of the PP powder, during the sonication used for coating. Even if the extent of agglomeration is the same in both types of graphite, the area of PP left uncoated will be larger in case of xGnP-15 so a higher concentration of xGnP-15 is required to reach percolation. Once the PP powder is completely covered by graphite then xGnP-15 can result in higher values of electrical conductivity as shown by comparison of the 0.5 vol% data points of Fig. 11.

Based on Fig. 11 it is clear that use of a slow cooling rate results in a lower percolation threshold and higher electrical conductivity for xGnP/PP nanocomposites. In order to understand the mechanism behind the cooling rate effect, the crystallization behavior of xGnP-1/PP and xGnP-15/PP at loadings of 0.1 and 0.3 vol% was studied by DSC using conditions that simulate the fast and slow cooling rates employed during compression molding.

As shown in Table 3 the temperature at which the crystallization starts (during the cooling cycle) is higher by ~20 °C in the case of the slow cooled samples for both the neat PP and the xGnP/PP composites. The higher crystallization temperature leads to larger spherulite size as shown in Fig. 3 where a comparison of the spherulites formed isothermally at $T = 130$ °C is provided. Thus it is concluded that the slow cooling rate leads to larger spherulites.

The degree of crystallinity is also presented in Table 3. For the neat polymer the slow cooling rate results in ~10% higher crystallinity compare to the fast cooled samples. However, the effect of cooling rate diminishes upon addition of any size of xGnP. Since slow cooling results in larger spherulites and since the degree of crystallinity is the same for both the slow and the fast cooled samples it is concluded that the slow cooling rate yields composites with lower percolation threshold that contain larger but fewer spherulites.

The melting enthalpy of the slowly cooled samples compared to the fast cooled specimens, shown in Table 3, indicates that the spherulites are thicker and larger. This is in agreement with the observation made in a study on isotactic PP reported that higher crystallization temperatures lead to thicker crystals [10]. The fast cooled samples have slightly higher melting temperatures (Table 3), estimated as the maximum of the melting peak with the DSC runs, which can be attributed to the melting of crystals formed by recrystallization during the reheating process [38].

XRD patterns of neat PP, xGnP-1/PP and xGnP-15/PP at reinforcement content of 0.1, 0.3 and 0.5 vol% made by coating and compression molding using the slow and fast cooling rates were obtained in order to investigate any correlation between the diffraction peaks and the percolation threshold of the composites. Representative results are shown in Figs. 12 and 13. Two and in some cases three

Table 3 Effect of cooling rate on the crystallization temperature, degree of crystallinity, melting enthalpy and melting temperature of xGnP/PP

Vol% xGnP	T_{crys}		x%		ΔH_{melt}		T_{melt} (°C)	
	SC	FC	SC	FC	SC	FC	SC	FC
0.0 xGnP	128.1 ± 0.2	109.2 ± 0.7	65.8 ± 0.9	59.2 ± 1.4	83.5 ± 3.4	64.0 ± 5.9	164.8 ± 0.1	168.3 ± 0.3
0.1 xGnP-1	136.9 ± 0.1	116.0 ± 1.1	63.9 ± 3.3	62.1 ± 1.5	87.1 ± 6.9	50.7 ± 6.1	167.5 ± 0.1	168.8 ± 0.2
0.3 xGnP-1	137.0 ± 0.1	116.0 ± 2.1	64.5 ± 2.2	63.5 ± 1.2	84.7 ± 3.1	55.9 ± 3.7	167.5 ± 0.2	168.7 ± 0.1
0.1 xGnP-15	136.4 ± 0.2	116.8 ± 1.6	60.5 ± 1.5	62.8 ± 0.4	79.9 ± 5.2	59.9 ± 3.3	167.4 ± 0.8	168.8 ± 0.1
0.3 xGnP-15	136.2 ± 0.3	116.7 ± 1.6	63.8 ± 1.5	62.5 ± 0.2	91.6 ± 1.2	57.2 ± 2.4	167.2 ± 0.2	168.7 ± 0.1

SC, slow cooling; FC, fast cooling

samples were studied for each condition (type and loading of reinforcement and cooling rate). There are six main peaks in all of the XRD patterns obtained that correspond to α-form crystals. One of the peaks, at $2\theta \cong 21°$, can either reflect the α-form crystal that appears at $2\theta = 21.2°$ and reflects the ⟨111⟩ plane or the β-form at $2\theta = 21.2°$ corresponding to the ⟨301⟩ plane. However, due to absence of the most dominant β-form peak at $2\theta = 16.8°$ it is assumed that the peak corresponds to the α-form crystal.

Only in case of the neat polymer as shown in Fig. 12 is there evidence of β-form crystals based on the weak peak at $2\theta = 16.8°$ which however disappears upon addition of xGnP. The reason is that since xGnP is a nucleating agent it increases the crystallization temperature as shown also in Table 3. In addition, according to a time–temperature-crystallization diagram for iPP [4] it is expected that only α-phase crystallites will be present since they form first at higher temperatures and if they grow too fast (in case of slow cooling) or the cooling rate is too high (case of fast cooling) the β-form crystals cannot form.

At slow cooling rates the XRD peaks are sharper and well defined whereas fast cooling rate results in samples with wider and weaker XRD peaks. In addition, as the xGnP content increases the peaks at $2\theta = 16.95°$ and $2\theta = 25°$, which correspond to the ⟨040⟩ and ⟨060⟩ crystallographic planes, are enhanced which is attributed to the nucleating effect of xGnP, ⟨002⟩ plane, as discussed previously. The observed increase in FWHM for the fast cooled samples indicates overall reduction of the crystallite size, which is also supported by DSC (Table 3).

Representative results presented in Figs. 14, 15 and 16, show the crystal thickness of neat PP, 0.1 vol% xGnP-15/PP and 0.5 vol% xGnP-15/PP, respectively. As mentioned above, β-form crystals exist only in case of neat polymer and in particular of those samples made by fast cooling as shown in Fig. 14. The β-form crystals are twice as large as compared to the α-form, which is in agreement with a study reporting that the lamellae of β-form PP (20 nm) are thicker than those of α-form PP (10 nm) [8]. The difference

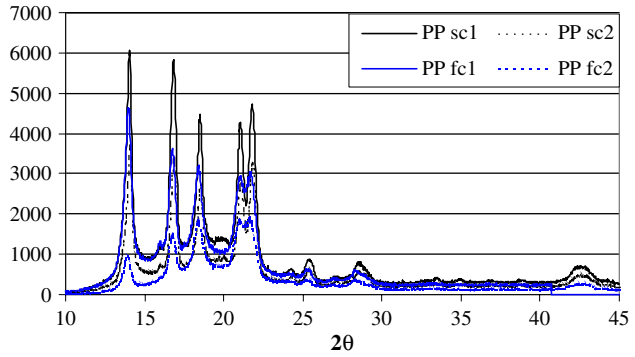

Fig. 12 XRD pattern of slow and fast cooled polypropylene (PP)

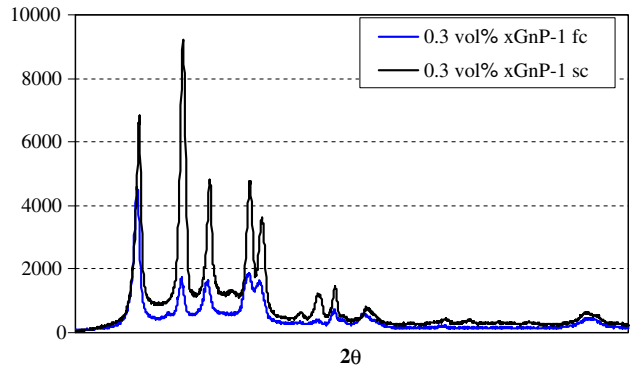

Fig. 13 XRD pattern of slow and fast cooled 0.3 vol% xGnP-1/PP

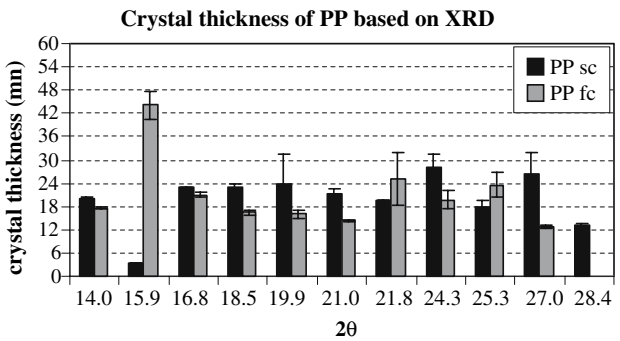

Fig. 14 Crystal size of polypropylene (PP) based on XRD

in the absolute value of the crystal thickness between the experimental data and the literature may be due to processing method and conditions used to fabricate the samples and the value assumed for the shape factor used in Eq. 2.

The arrows in Fig. 15 indicate the crystal size corresponding to the six main XRD peaks. In most cases the slow cooling results in thicker crystals and the difference becomes larger upon addition of xGnP as shown in Figs. 15 and 16. The question as to why the slow cooling compared to fast cooling and the smaller aspect ratio graphite, xGnP-1, compared to xGnP-15 result in composites with lower percolation threshold can be answered by taking into consideration and combining all the results presented in this section. Based on Figs. 15 and 16 it is evident that fast cooling results in crystals that are ~20–30% thinner compared to the crystals formed during slow cooling of the composites. According to Table 3 the degree of crystallinity is the same for both the slow and the fast cooled samples, thus it is concluded that slow cooling results in larger but fewer crystals.

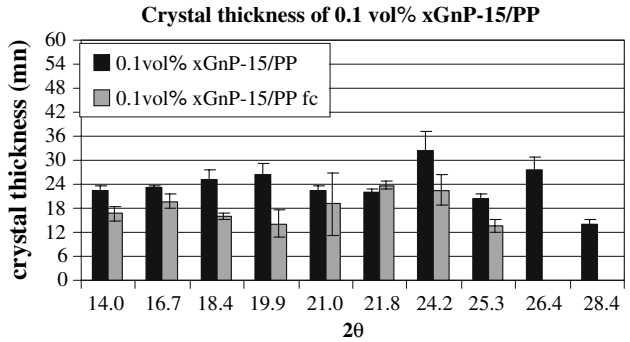

Fig. 15 Crystal size of 0.1 vol% xGnP-15/PP based on XRD

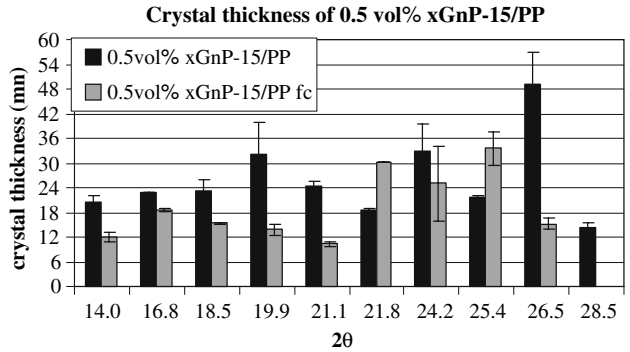

Fig. 16 Crystal size of 0.5 vol% xGnP-15/PP based on XRD

As indicated by DSC and optical microscopy, xGnP is a nucleating agent for PP and the crystals are growing around the platelets. In the case of fast cooling there are more crystals so a larger number of graphite platelets will be in inside the crystals and fewer will be available to form the continuous network necessary for providing electrical conductivity as compared to the slow cooled samples. In addition, the conductive path of xGnP can be disrupted by the presence of many small spherulites that exist in the fast cooled composites. Thus a higher loading of xGnP, which means higher percolation threshold, is required to impart the electrical conductivity of the composites in case of fast cooling.

The same argument can also explain why xGnP-1 has a lower percolation threshold. At the same specific volume loading, xGnP-1 has more platelets than xGnP-15. Additionally, xGnP-15 tends to agglomerate more and thus the number of platelets available to form the conductive path is further reduced. However, once the conductive path is formed then the electrical conductivity of xGnP-15/PP is higher (10^{-3} S/cm at 0.5 vol%) compared to xGnP-1/PP (10^{-4} S/cm at 0.5 vol%), which reflects the effect of the aspect ratio and size.

The mechanism described above is summarized schematically in Fig. 17. Both the slow and the cooled samples shown in Fig. 17a, b, respectively contain the same amount

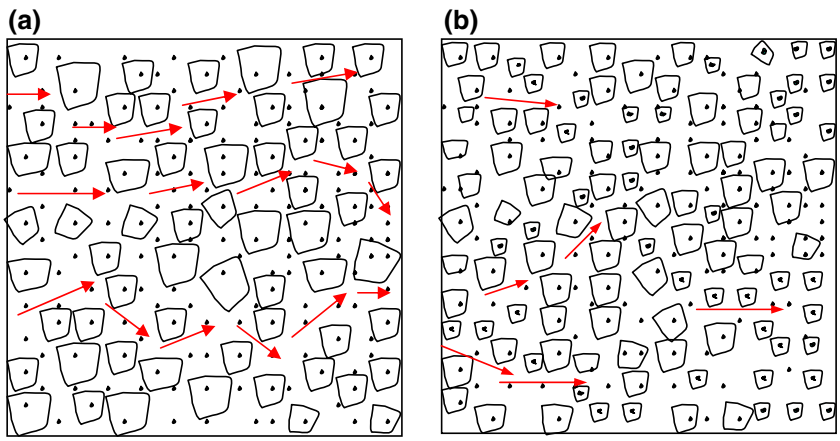

Fig. 17 Schematic of the microstructure of premixed compression molded xGnP/PP (**a**) slow cooled and (**b**) fast cooled. The *arrows* indicate the formation of conductive network which can span across the whole sample in case of slow cooling

of reinforcement (black spots). The PP crystals grow around the xGnP in both cases. The basic difference is that in the slow cooled sample there are fewer but (20–30%) larger crystals and the number of xGnP available to form the conductive path, which is indicated by the red arrows, is higher.

Conclusions

The effect of xGnP on the crystallization behavior of PP was investigated using optical microscopy, DSC and XRD. It was found that xGnP, even at loadings as low as 0.01 vol%, is a nucleating agent for PP and increases the crystallization temperature (during the cooling cycle) and the crystallization rate. No effect on the degree of crystallinity was observed and the number of nucleation sites increases with the concentration of any type of xGnP.

Additionally it was concluded that xGnP can induce the nucleation of the β-form PP crystals which have higher impact strength compared to the most common α-form PP crystals. A saturation effect on the nucleation of β-form crystals was observed at higher xGnP concentrations (1 vol% for xGnP-1 and $\sim$10 vol% for xGnP-15) which is attributed to the fact that there is not enough polymer to penetrate between the platelets and keep them apart leading to poor dispersion that does not utilize the xGnP surface that is available for crystal nucleation.

According to the XRD results, the nucleating efficiency of xGnP can be also expressed as the change in the intensity ratio between the α-form (040) and (110) reflections and/or as the enhancement of peaks that correspond to crystallographic planes of the general (00α) type which is attributed to the alignment of PP chains along the xGnP surface and epitaxial crystal growth due to crystallographic match between these PP planes and the graphite's (002) plane.

The relationship between crystallinity and percolation threshold/electrical conductivity of xGnP/PP nanocomposites was also investigated. The crystallization of the matrix was altered by cooling the composites at different rates once the molding was completed. It was found that fast cooling results in composites with higher percolation threshold. In the fast cooled composites there are more but smaller/thinner crystals, hence more graphite platelets are inside the crystals and thus fewer available to form the conductive path. In addition the more and smaller crystals may disrupt the formation of the conductive network thus increasing the percolation threshold. It was also found that xGnP-1 has a lower percolation threshold (10^{-6} S/cm at 0.1 vol%) compared to xGnP-15 (10^{-3} S/cm at 0.5 vol%) which is also attributed to the larger number of xGnP-1 that are contained in a given xGnP loading and to the fact that xGnP-15 agglomerate more and thus the number of platelets available to form the conductive path is further reduced.

Overall, it is concluded that the presence of xGnP significantly alters the crystallization behavior of PP and by using the proper processing conditions the properties of xGnP/PP such as impact strength, percolation threshold and electrical conductivity can be strongly affected. Finally, it has been shown that due to the nucleating effect of xGnP and the resulting crystalline structure of PP, the number of xGnP platelets has a stronger effect on the percolation threshold of xGnP-PP nanocomposites than their aspect ratio.

Acknowledgements Partial support for this research was provided by a grant from NASA LaRC, "Graphite Nanoreinforcements for Aerospace Nanocomposites" NAG1-01004, Thomas Gates, Program Director. The authors also wish to express their thanks to the Basell Chemical Company for providing the polypropylene resin.

References

1. Klijusuric JG (2003) Sadhana 28:991
2. Chaiko DJ, Leyva AA (2005) Chem Mater 17:13
3. Huy T, Adhikari R, Lupke T, Henning S, Michler G (2004) J Polym Sci B Polym Phys 42:4478
4. Zheng W, Lu X, Toh CL, Zheng TH, He C (2004) J Polym Sci B Polym Phys 42:1810
5. Karger-Kocsis J, Varga J, Ehrenstein GW (1997) J Appl Polym Sci 64:2057
6. Karger-Kocsis J (1996) Polym Eng Sci 36:203
7. Karger-Kocsis J, Varga J (1996) J Appl Polym Sci 62:291
8. Li JX, Cheung WL (1998) Polymer 39:6935
9. Park S-Y, Cho Y-H, Vaia RA (2005) Macromolecules 38:1729
10. Devaux E, Bourbigot S, Achari A-E (2002) J Appl Polym Sci 86:2416
11. Nair SS, Ramesh C (2005) Macromolecules 38:454
12. Maiti P, Okamoto M (2003) Macromol Mater Eng 288:440
13. Bhattacharyya AR, Sreekumar TV, Liu T, Kumar S, Ericson LM, Hauge RH, Smalley RE (2003) Polymer 44:2373
14. Grady BP, Pompeo F, Shambaugh RL, Resasco DE (2002) J Phys Chem B 106:5852
15. Valentini L, Biagiotti J, Lopez Manchado MA, Santucci S, Kenny JM (2004) Polym Eng Sci 44:303
16. Gopakumar TG, Page D (2004) Polym Eng Sci 44:1162
17. Sherman LM (2006) Chasing nanocomposites. Plastics technology. http://www.plasticstechnology.com as on 10 February 2006
18. Banerjee P, Mandal BM (1995) Macromolecules 28:3940
19. Jing X, Zhao W, Lan L (2000) J Mater Sci Lett 19:377
20. Bigg DM (1984) Adv Polym Tech 4:255
21. Gokturk HS, Fiske TJ, Kalyon DM (1993) J Appl Polym Sci 50:189
22. Fiske TJ, Gokturk HS, Kalyon DM (1997) J Mater Sci 32:5551
23. Shen JW, Chen XM, Huang WY (2003) J Appl Polym Sci 88:1864
24. Chen XM, Shen JW, Huang W-I (2002) J Mater Sci Lett 21:213
25. Heiser JA, King JA, Konell JP, Sutter LL (2004) Adv Polym Tech 23:135
26. Chen G-H, Wu D-J, Weng W-G, He B, Yan W-L (2001) Polym Int 50:980

27. Chen G-H, Wu D-J, Weng W-G, Yan W-L (2001) J Appl Polym Sci 82:2506
28. Chodak I, Omastova M, Pionteck J (2001) J Appl Polym Sci 82:1903
29. Chodak I, Krupa I (1999) J Mater Sci Lett 18:1457
30. Valentini L, Biagiotti J, Kenny JM, Lopez-Manchado MA (2003) J Appl Polym Sci 89:2657
31. http://www.dow.com/polyolefins/about/pptechctr/primer/typical.htm as on 1 October 2006
32. http://www.graphtech.com as on 20 October 2006
33. Fukushima H (2003) PhD thesis, Michigan State University, 2003
34. Reynolds WN (1968) Physical properties of graphite. Elsevier Publishing Co. Ltd, p 1
35. Kalaitzidou K (2006) PhD thesis, Michigan State University, 2006
36. Nuffield EW (1966) X-ray diffraction methods. Wiley, New York
37. Chen J-H, Tsai F-C, Nien Y-H, Yeh P-H (2005) Polymer 46:5680
38. Supaphol P, Spruiell JE (2000) J Appl Polym Sci 75:44
39. Zheng Q, Shangguan Y, Yan S, Song Y, Peng M, Zhang Q (2005) Polymer 46:3163
40. Ferrage E, Martin F, Boudet A, Petit S, Fourty G, Jouffret F, Micoud P, De Parseval P, Salvi S, Bourgerette C, Ferret J, Saint-Gerard Y, Buratto S, Fortune JP (2002) J Mater Sci 37:1561
41. Chung D (2002) J Mater Sci 37:1475
42. Calvert P (1999) Nature 399:210